Contents lists available at ScienceDirect

Ceramics International

Catalytic graphitization of novolac resin for refractory applications

S.I. Talabi[a,b,*], A.P. Luz[a], A.A. Lucas[a], C. Pagliosa[c], V.C. Pandolfelli[a]

[a] Federal University of São Carlos, Materials Engineering Department, Rod. Washington Luiz, km 235, São Carlos, SP 13565-905, Brazil
[b] University of Ilorin, Materials and Metallurgical Engineering Department, PMB 1515, Ilorin, Kwara State, Nigeria
[c] RHI-Magnesita, Research and Development Center, Praça Louis Ensch, 240 Contagem, MG, Brazil

ARTICLE INFO

ABSTRACT

This study investigated how to induce graphite generation from the carbonization process of novolac resins using conditions that can be adopted for carbon-containing refractories (CCRs) production. The effect of boron oxide or boric acid (graphitizing agents), cross-linking additive (hexamethylenetetramine) and some processing parameters (mixing technique, vacuum degassing, heating rate and thermal treatments) on carbon graphitization from a commercial novolac resin were evaluated. The X-ray diffraction (XRD) technique was selected to measure the graphitization level and crystal parameters of the prepared samples. Based on the attained results, adding graphitizing agents prior to the pyrolysis of resin resulted in carbon crystallization. The best graphitization level was obtained when the mixtures containing 6 wt% B_2O_3 or 10 wt% H_3BO_3 were fired up to 1000 °C for 5 h using a heating rate of 3 °C/min. Although the reproducibility of the obtained results was ascertained, heterogeneous graphitization could be observed based on the XRD profiles, as well as some discrepancies in the calculated graphitization level values. This phenomenon was attributed to the additives susceptibility to agglomeration, preferential graphitization starting from lower binding energy sites and heat treatment temperature, among others.

1. Introduction

Carbon-containing refractories present special thermomechanical properties, which depend on the presence of graphite in their formulation. Although polymeric materials are commonly classified as non-graphitizable organic precursors, the product from carbonization of thermosetting resins (which are the most common binder compounds used in such compositions) might provide an additional source of crystalline carbons in the resulting microstructure.

Novolac (Nv) and resole (Rs) resins have gained popularity as choice binders to develop CCRs, such as MgO-C bricks. These thermosetting compounds act enhancing the refractories' green mechanical strength, thermal shock resistance and reduce porosity levels [1]. Furthermore, they induce minimal emissions of polycyclic aromatic hydrocarbons and other toxic substances during their pyrolysis, thereby providing greater environmental health benefits [2,3]. Despite this, the poor oxidation resistance and non-graphitizability of carbons derived from resins are still limited in terms of their usefulness in the development of refractory products for high temperature applications [4].

Unaided pyrolysis of Nv is a solid state process without the formation of liquid or semi-liquid components, which yield non-graphitic carbons. Phenolic resin has been considered a non-graphitizable

material as it goes through the mesophase stage during thermal treatment and results in what is regarded as hard carbons. Various methods based on the application of compressive force, magnetic field, radiation, etc., have been used to induce the conversion of disordered-hard-carbons from its pyrolysis into crystalline ones [5–7]. However, the most successful technique for CCR development may entail using graphitizing additives in a process called catalytic graphitization [8]. This approach leads to the transformation of amorphous carbon (from novolac or resole resins) to the graphitic type during carbonization in the presence of those elements or compounds, at lower temperatures and shorter heat treatment time (HTT). Some elements (e.g., nickel, boron), organometallics (e.g., metallocenes, benzoates, octoates and naphthenates), metal oxides, etc., are found to be suitable graphitizing agents for disordered carbons as they can speed up the generation of the graphite phase at high temperatures [9–13].

Recently, boron-based additives have received considerable attention due to their ability to act as antioxidant agents for CCRs, preventing carbon oxidation when heated in an oxidizing environment. These compounds give rise to liquid B_2O_3 in the designed microstructure, which coats the carbon surface and limits its oxidation resulting in increased char yield [14–18]. Moreover, as reported in various papers, phenylboronic acid [16], boric acid [17,19,20],

---

hyperbranched polyborate [21], boric acid terminated hyperbranched polyborate [22], bis(benzo-1,3,2-dioxaborolanyl)oxide [23], bis (4,4,5,5-tetramethyl-1,3,2-dioxa-borolanyl)oxide [23], boron carbide [24–26] etc., have been used to induce some degree of graphitization in Nv. The actual mechanism of the proposed reactions is not yet clear. However, the graphitizing effect of boron sources can be examined from various perspectives and each of the reaction pathways outlined below may be interrelated:

i. *Formation-Decomposition*: B-C bond is formed during carbonization of the cured modified resin at temperatures above 500 °C [17,27]. The cleavage of boron-carbide phase during pyrolysis leads to the generation of graphite. Generally, sp^2 carbons are more stable than sp^3 ones and reordering the atoms leads to crystalline carbon formation (the standard enthalpy change of graphite formation is 0 kJ/ mol [7]). However, this change is generally slow at room temperature due to the number of bonds necessary to be broken in the process.

ii. *Dissolution-Precipitation*: The presence of boron compounds favors the formation of liquid B_2O_3 (melting point = ~ 450 °C) and this phase acts as a solvent for carbon, resulting in graphite crystallization. During the process, the B-O-C bond breaks above 800 °C [16,17]. The formation of B-O-C (190.2 eV [17]) and B-C (189 eV [27]) bonds with a lower binding energy than plain C-C (284.8 eV) ones, which characterized the uncatalyzed resin, may allow the disruption and structuring needed for graphite generation at lower temperatures.

iii. Incorporation of boron atoms via substitution during pyrolysis of the catalyzed resin can lead to increased orderliness of the carbon structure, as they may slip within the layer of the pre-existing carbons without completely disrupting it [17,28,29]. Moreover, boron has been reported to have the ability of entering the interstitial sites of carbon lamellar structure [11].

The postulations outlined above indicate that boron-based additives provide active sites for the rearrangement of amorphous carbon produced during pyrolysis of the catalyzed resin by reducing the reaction barrier for their transformation to graphitic ones.

The primary objective of most of the published research studies on the use of boron-based additives involved the development of carbon-carbon composites with improved thermal resistance. However, less attention has been focused on the applicability of such methods in the development of carbon-containing refractories. In this study, the influence of several processing parameters and catalytic additives on the generation of graphitic carbons from a commercial novolac resin was investigated. It is believed that the knowledge attained will provide a path to achieve in-situ graphitization of novolac resin binders in CCRs.

2. Methodology

Commercial novolac resin (Nv, Prefere® 88 5010R), which is commonly used as a refractory binder, was analyzed in this study. Boron-containing compounds (B_2O_3 and H_3BO_3) were selected as the likely graphitizing agents. To ensure proper comparison, the resulting content of boron oxide in the compositions containing H_3BO_3 or B_2O_3 was equivalent to 6 wt%. General information about the raw materials and sample formulations is presented in Table 1.

Firstly, the compositions were mixed at room temperature for 20 min in a mechanical stirrer (rotation speed of 300 rpm) to obtain dispersion of the additives within the novolac resin. Thereafter, each of the prepared mixtures was poured into alumina crucibles, covered with alumina disks and embedded in a refractory box filled with coke to create a reducing environment during pyrolysis and thermal treatments. The samples were subjected to different heating sequences designated as A2-A5, B3 and C3-procedures (see Table 2). The A-procedure consisted of heating the formulation to 100 °C and keeping it at

Table 1
General information about raw materials and description of samples.

Materials	Main Features	Supplier
Novolac resin	Nv, Liquid (solvent = ethylene glycol) Density = 1.18 g/cm^3	Dynea, Brazil
Boron oxide	B_2O_3, solid powder, (d_{50} < 10 μm, 99% purity)	Magnesita Refratários SA
Boric acid	H_3BO_3, solid powder, molecular weight = 61.83, Product code: A1025.01A4, (d_{90} < 45 μm, 99%)	Synth Chemical Co., SP-Brazil
Hexamethylenetetramine	HMTA, solid powder	Dynea, Brazil
Evaluated Compositions	**Description**	
Nv-HMTA (reference sample)	Nv + 10 wt% HMTA	
Nv-6B	Nv + 6 wt% B_2O_3	
Nv-10H	Nv + 10 wt% H_3BO_3	
Nv-HMTA-6B	Nv + 10 wt% HMTA + 6 wt% B_2O_3	
Nv-HMTA-10H	Nv + 10 wt% HMTA + 10 wt% H_3BO_3	

that temperature for 4 h, followed by further heating at 500 °C for 1 h and finally at 1000 °C for 5 h. The firing sequence was chosen to induce the dispersion, carbonization and graphitization of additives, respectively. The heating rates varied from 2 to 5 °C/min and subsequently cooled to room temperature (30 °C) at a rate of ~16 °C/min. In the B and C-procedures, the heat treatments were modified by introducing more steps at the curing stages. For instance, the samples were kept at 80 °C for 4 h, followed by a dwell time of 1 h at 100 °C and 30 min at 150 °C before the carbonization/graphitization stages for the B-procedure, whereas the other treatment (C-procedure) consisted of heating up the materials to 100 °C for 2 h, followed by an additional step at 220 °C for 1 h. The heating modification provides the opportunity to study the effect of curing steps on crystallization of the catalyzed resin carbons. Both B3 and C3-procedures were carried out at a heating rate of 3 °C/min and cooled at ~16 °C/min. Furthermore, the effect of additional ultrasonic mixing for 30 min, vacuum degassing for 15 min, cross-linking agent (hexamethylenetetramine) on the graphitization process were investigated in the course of the experiments (see Table 2).

Subsequently, the carbon samples were primarily ground in a vibratory mill for 12 s before characterization via X-ray diffraction (XRD). The experiments and analysis were repeated several times to ascertain reproducibility and a homogeneous level of the attained graphitization. The XRD analysis was carried out using Rigaku Geigerflex equipment with graphite monochromator under CuKα radiation [λ = 1.5418 Å, scanning step = 0.032°] to determine the graphitization level and for phase identification of the pyrolytic products. OriginPro lab-9 software was used to quantify the amount of generated crystalline carbons according to the procedure proposed by Bitencourt et al. [8]. The simulation presented a root mean square value (R^2) greater than 0.9. Before iterations, the following mathematical functions were defined for the different peaks: (i) Gaussian function was used for the graphitic phase peak and crystalline phases (ii) asymmetric double sigmoidal (Asym2Sig) function for the peak at ~24°.

After simulation, the graphitization level (GL) was calculated using Eq. (1). The total area related to the peaks of graphitic carbons was divided by the sum of the peaks related to graphitic and non-graphitic carbons. The area related to the minor peaks associated with the presence of impurities such as tungsten carbide was not considered in the determination of the GL values.

$$Graphitization\ level\ (GL) = \frac{Graphitic\ carbon\ area}{Total\ area\ (graphitic\ carbon + non-graphitic\ carbon)} \quad (1)$$

OriginPro lab-9 software was also used for deconvolution of the diffractogram in the 20–32° of 2θ region in order to determine the

Table 2
Details of the heating steps and mixing techniques carried out to induce the graphitization of resin.

Designation	Heat Treatment Description	Heating rate
A2-A5 procedure	100 °C / 4 h + 500 °C / 1 h + 1000 °C / 5 h (Note: the number after the letter describes the heating rate i.e. A3 implies the formulation was subjected to thermal treatment using A-procedure at a heating rate of 3 °C/min)	2–5 °C/min
B3-procedure	80 °C / 4 h + 100 °C / 1 h + 150 °C / 30 min + 500 °C / 1 h + 1000 °C / 5 h	3 °C/min
C3-procedure	100 °C / 2 h + 220 °C / 1 h + 500 °C / 2 h + 1000 °C / 5 h	3 °C/min
Mixing Procedures	**Description**	
M	Mechanical mixing	
M-V	Mechanical mixing + vacuum degassing	
M-U	Mechanical mixing + ultrasonic mixing	

interlayer spacing and crystallite height. These parameters were calculated using Eqs. (2) and (3), respectively.

$$n\lambda = d_{200} \, 2 \sin \theta \qquad (2)$$

$$k\lambda = L_c \beta \cos \theta \qquad (3)$$

where n = positive integer, d_{200} (nm) = interlayer spacing, θ = incident angle, L_c (nm) = crystallite height and k = 0.89.

3. Results and discussion

3.1. Effect of B_2O_3 and H_3BO_3 on carbonized novolac resin graphitization

Crystallinity and structural orderliness of the pyrolyzed samples were studied using X-ray diffraction technique. Fig. 1 shows the XRD pattern of the pyrolytic carbon produced from a mixture of novolac and 10 wt% HMTA (reference sample) and fired using A3-procedure. The profile was characterized with a low intensity broad hump between 20° and 30° near the 002 plane of the graphitic structure. The peak at ~43° corresponds to 100 in-plane symmetry for turbostratic graphitic structure. This is the typical diffractogram of sp³-hybridized carbons with an amorphous structural arrangement based on a rigid structure (π-bonds) that limits the rotation of atoms to graphene layers during pyrolysis [30]. Similarly, carbonized Nv without HMTA addition presents the same XRD pattern. Based on this result, graphitization of plain novolac resin was not favoured at 1000 °C. Furthermore, research findings have shown that higher processing temperatures (1650–1750 °C) used in steel making is not sufficient for crystallization of carbon from such organic resin [31]. In fact, the highly cross-linked nature of Nv carbons should inhibit thermal ordering even at temperatures up to 3000 °C [32]. The additional peaks observed at 31.5°, 35.5° and 48° (Fig. 1) are related to tungsten carbide contamination from the grinding equipment lining material, used for samples preparation for analysis.
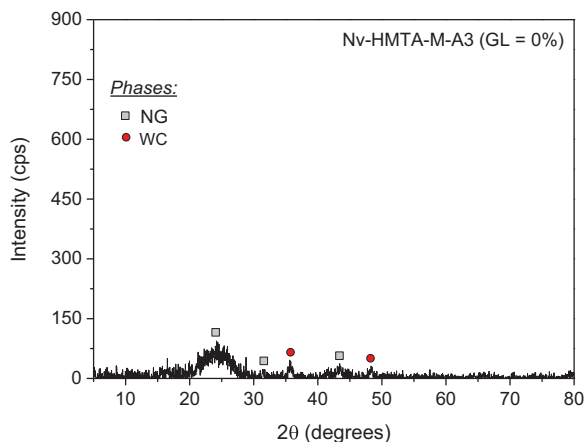

Fig. 1. X-ray diffraction pattern of novolac resin + 10 wt% HMTA (reference composition) after firing at 1000 °C for 5 h using A3-procedure (NG = non-graphitic, WC = tungsten carbide, GL = graphitization level, M = mechanical mixing).
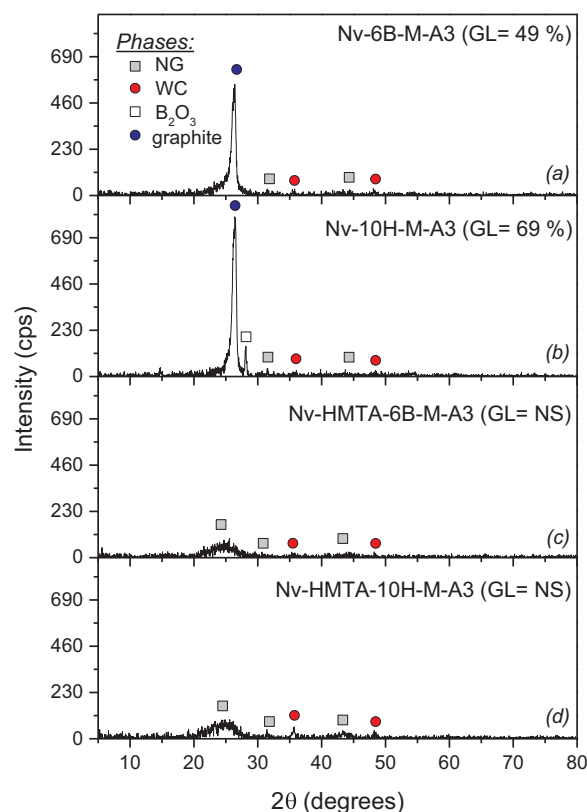

Fig. 2. XRD profiles showing the effect of boron-based additives on graphitization of a commercial novolac resin (with and without 10 wt% HMTA) after firing at 1000 °C for 5 h under reducing atmosphere. GL = graphitization level, NS = not significant, A3 = heating procedure at 3 °C/min, M = mechanical mixing, NG = non-graphitic, WC = tungsten carbide, 6B = 6 wt% B_2O_3, 10 H = 10 wt% H_3BO_3, HMTA = 10 wt% hexamethylenetetramine.

Despite the non-graphitizing characteristic of novolac resin (as observed in Fig. 1), the XRD profiles of carbons from the catalyzed resin (containing B_2O_3 or H_3BO_3) show a transition from highly amorphous to graphitic ones. The diffractograms of Nv-6B-M-A3 (Fig. 2a) and Nv-10H-M-A3 (Fig. 2b) show an asymmetric 002 peak at ~26°, which gets sharper and with increased intensity due to the stacking of graphene layers. The intensity and width of the graphite peak at ~26° are generally used to explain carbon graphitization [8,17,19]. These results agree with earlier observations by other researchers that the incorporation of boron enhances crystallization of pyrolyzed organic precursors [17,33].

Moreover, the observation is significant as graphitization is normally not achieved at such temperatures (1000 °C). A new distinct peak (at ~28°) corresponding to the B_2O_3 phase was also identified in the Nv-10H-M-A3 composition (Fig. 2b). Although some authors [17,21,34] reported the volatization of boron oxide after heating at 1000 °C, its presence suggested that oxygen may have partially

participated in the pyrolysis because coke (instead inert gas) was used to create the reducing environment during the samples' treatment [8]. However, as this phase was only detected in compositions prepared from boric acid catalyzed resin, its presence may also be attributed to the additional reaction-step involving initial formation and decomposition of phenylborate (formed during the curing of novolac resin [17]) to boron oxide at 400 °C. Nevertheless, the presence of B_2O_3 may be beneficial in the refractory material formulation (such as MgO-C), as it can lead to the formation of a low melting phase $(3MgO.B_2O_3)$ that can block open pores and coat the carbon surface, thus suppressing oxidation. However, this benefit will be at the expense of hot mechanical strength. The graphitization level (GL) of Nv-6B-M-A3 and Nv-10H-M-A3 samples was calculated to be 48.8% and 68.7%, respectively (Figs. 2a and 2b).

Besides that, the influence of HMTA (which is a hardener agent used in the development of resin-bonded refractories to increase its amount of fixed carbon yield [35]) addition to the formulations, was also evaluated. By incorporating 10 wt% HMTA to either boron oxide or boric acid catalyzed resin, the graphitization was inhibited (Figs. 2c and 2d). Heteroatoms, such as nitrogen and its functional groups (present in HMTA), typically enhance reactivity and cross-linking of atoms [36]. These reactions significantly reduced the graphitizability of the resultant carbons and prevented reconstructive transformation necessary for graphite generation. The results suggest that to achieve ordered arrangement, atoms' binding energy must be much weaker to allow carbon nuclei formed during the initial stages of carbonization to remain relatively mobile [37–39]. This inference was similar to the observation made by Kipling et al. [40–42] when studying the factors influencing graphitization of polymer carbons. The authors found that substantial cross-linking during the curing stages prevented the crystallization of carbons. The XRD profiles of the resulting samples were similar to those obtained by Yun et al. [43], with a novolac composition containing 12 wt% HMTA and phenylboronic acid. This observation was also reported by Luz et al. [44]. In this article, the authors realized 0% graphitization level after subjecting the formulation of novolac resin containing 10 wt% HMTA and 10 wt% boric acid to a heating sequence involving slow curing stage. Moreover, formulations prepared with a lesser amount of HMTA (1 or 5 wt%) also showed reduced likelihood to graphitization.

The experiments and XRD analysis were repeated six times for each composition to ascertain reproducibility of the obtained results using the mixtures that presented the best graphitization level. The calculated GL values are shown in Table 3. Most related studies published in the literature overlooked this important aspect (reproducibility). Therefore, based on the experimental results, the following conclusion/inferences were made:

i. The addition of boron containing compounds such as B_2O_3 and H_3BO_3 to novolac resin leads to its graphitization at 1000 °C.
ii. Graphitization of the boron-catalyzed novolac samples at 1000 °C takes place in a heterogeneous manner. The selected additives caused partial acceleration of the carbon matrix crystallization, producing carbons consisting of different phases (i.e. G = graphitic and T = turbostratic or non-graphitic components).
iii. The average GL value for Nv-10H-M-A3 is ~8% less than the one

Table 3
Graphitization level of the mixtures containing novolac resin + B (B_2O_3) or H (H_3BO_3) after heating up to 1000 °C/5 h under reducing atmosphere (average of 6 evaluations for 2 different batches for each composition).

Samples	GL_a (%)
Nv-6B-M-A3	47 ± 10
Nv-10H-M-A3	49 ± 12

obtained by Luz et al. [44] that used similar composition and experimental procedure. The calculated standard deviation results for this property indicate the heterogeneity of the attained samples.

The following are some likely reasons for the heterogeneous graphitization/limited reproducibility detected in the samples:

i. The agglomeration of additives as a result of their susceptibility to hydration (water vapour is released during the heat treatment process [45]) and the natural tendency for particles coagulation [24,46] can lead to heterogeneous graphitization and non-uniform distribution of the graphite phase. This observation agrees with the study carried out by Wang et al. [24], where B_4C particles were dispersed in phenolic resin with the aid of a powerful mixing device for 40 min. The inhomogeneous distribution and additive accumulation (even after heat treating the sample up to 300 °C) was attributed to the relatively high viscosity of phenolic resin and the difference in the physical properties of both materials [24].
ii. The incorporation of boron atoms or non-uniform distribution of residual B_2O_3 in the carbon matrix might lead to a peak broadening effect. As pointed out by Davor and Balzar, any lattice imperfection such as the presence of vacancies, dislocation, interstitial and similar defects can cause X-ray diffraction line broadening [47].
iii. Temperature is a key factor in thermosetting resin graphitization. As observed by Franklin [48], homogenous graphitization is a function of cross-linking developed between the carbon atoms (during the curing stage) and temperature at which pyrolysis was carried out. These observations agree with the results by Ōya et al. [11]. These latter authors reported that uniform and continuous graphitization of carbons derived from phenolic resin catalyzed with boron only begins at 1800 °C. Hence, to achieve continuous carbon crystallization, the maximum pyrolysis temperature must provide sufficient energy to break the maximum number of bonds.
iv. Another likely cause is the preferential graphitization originating from B-O-C sites with lower binding energy than C-C bonds (B-O-C band was detected in the FTIR profile of samples heat treated up to 230 °C or 500 °C). This type of mechanism has been observed in graphitization of thermosetting resin under a high pressure such as 1000 MPa. At that instant, heterogeneous crystallization was ascribed to the internal stress generated through anisotropic thermal expansion of carbon crystallites, concentrated at certain sites where graphitization proceeds preferentially in order to release the stress [49]. Such preferred graphitization of carbons derived from phenolic resins around pores was also implied in a study by Kamiya and Suzuki [50]. Microstructural examination shows packets of carbons around pores formed during the hardening and carbonization process. The concept suggests that increasing the amount of graphitizing agents may enhance the homogeneity/graphitization level. However, the fact that boric acid is sometimes used as a catalyst and hardening agent for thermosetting resin, such as novolac in the foundry industry, may not allow unlimited additions [46].

From the XRD characterization, structural features such as crystallite height (L_c) and interlayer spacing (d_{002}) of the graphitized carbons was determined using Scherrer's (Eq. (2)) and Bragg's (Eq. (3)) equations, respectively. Both parameters have been used to describe the degree of carbon crystallization, where an increasing L_c and decreasing d_{002} (tending towards 0.3354 nm, which is graphite's d_{002} value) indicate a higher graphitization level [17]. As mentioned earlier, OriginPro lab-9 software was used for the diffractogram deconvolution in the 20–32° of the 2θ region. To determine L_c and d_{002} parameters, the humps were fitted using Gaussian peaks. Table 4 shows the obtained results. As expected, a range of values was obtained for both evaluated properties due to the heterogeneous nature of the compositions. The carbon interlayer spacing values are in the range of 0.3372–0.3427 nm, whereas the crystallite heights are in the 7–12 nm one. Nevertheless,

Table 4
Crystal parameters of pyrolytic carbon samples fired at 1000 °C for 5 h under reducing atmosphere (for the composition without HMTA, the results represent the average and standard deviation of 6 measurements in 3 different batches).

Samples	L_c (nm)	d_{002} (nm)
Nv-HMTA-M-A3	1.69	$0.3629 - 0.3742$
Nv-HMTA-6B-M-A3	$2.06 - 2.78$	$0.3604 - 0.3606$
Nv-HMTA-10H-M-A3	$2.96 - 3.01$	$0.3608 - 0.3610$
Nv-6B-M-A3	9.39 ± 2.39	0.3406 ± 0.002
Nv-10H-M-A3	10.66 ± 2.09	0.3382 ± 0.001

these parameters are within the range obtained in the literature for carbonized novolac resin modified with boron-containing compounds [17,19,22,44], which suggests a random combination of graphitic and turbostratic stacking [51].

However, a significant increase in L_c detected in some of the compositions show that boron catalyzed the process resulting in some degree of orderliness [52]. As reported by some authors [17,53], the incorporation of boron can bring about change in π-electron density, which could result in reduced interlayer spacing and increased crystallite height. Specifically, the presence of boron in the carbon matrix can lead to electron deficiency and more attractive interaction between the π-electron clouds of adjacent graphitic layers allowing them to come closer together [22,54]. Boron atoms have the ability to intercalate carbons during pyrolysis of the catalyzed resin [28,55]. Their enhanced diffusivity also allow them to act as vacancies in carbon structure, which favors the growth of L_c and reduced d_{002} [33]. Furthermore, as the growth of crystals in the c-direction requires good planer stacking, there is an agreement between the increased values of L_c (compared to the reference composition) and those of d_{002} with estimations closer to graphene layers [56].

It is important to highlight that the effect of grinding time (using a WC lined mill) when preparing the samples for XRD analysis (up to 120 s) was studied as an alternative way to effectively quantify the amount of generated graphite. A more representative composition which presents about 3–7% difference in graphitization level values was obtained (XRD profiles not presented here). However, while increased grinding time effectively led to the samples' homogeneity, it also caused significant amorphization. Notably, the peak intensity at 31.5°, 35.5° and 48° related to tungsten carbide contaminant from the grinding equipment lining material also increased with prolonged milling. Consequently, this method was considered not reliable compared to determining the average graphitization level. Moreover, the GLa (average graphitization level) values provide a basis to identify other factors that can influence the catalyzed resin graphitization.

3.2. Influence of processing parameters while preparing the mixtures

Based on the attained results, an attempt was made to study the influence of other processing parameters on the graphitization behavior of the catalyzed novolac resin. Taking this into consideration, the use of ultrasonic mixing, vacuum degassing, heating rates and heat treatment sequence were investigated. Higher mixing speed and time were not analyzed in the present work because, based on the observation of other researchers, the following can be stated: (i) prolonged mixing/agitation may lead to heat generation, which most likely limits the degree of graphitization of resins [44] (ii) particle agglomeration can be detected even after prolonged mixing (40 min) of phenolic resin and boron carbide additives at room temperature [24].

3.2.1. Effect of additional ultrasonic mixing on the graphitization level

Research studies have shown that to achieve effective carbon crystallization derived from phenolic resins, the additives should be properly dispersed within the composition's matrix [8]. Based on this information, ultrasonic mixing was incorporated into the preparation
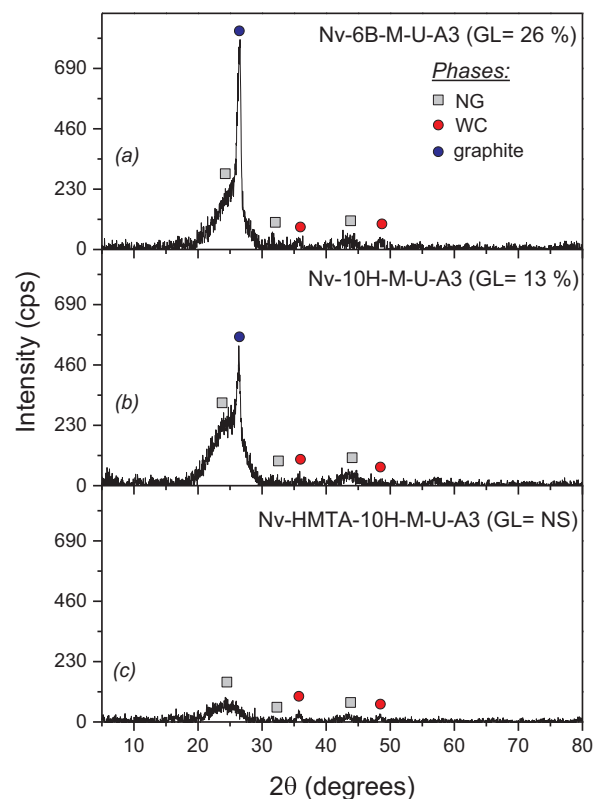

Fig. 3. XRD profiles of the prepared samples showing the effect of additional ultrasonic mixing on catalytic graphitization of novolac resin after firing at 1000 °C for 5 h under reducing atmosphere. GL = graphitization level, NS = not significant, A3 = heating procedure at 3 °C/min, M = mechanical mixing, U = ultrasonic mixing, NG = non-graphitic, WC = tungsten carbide, 6B = 6 wt% B_2O_3, 10 H = 10 wt% H_3BO_3, HMTA = 10 wt% hexamethylenetetramine).

procedures. Compared to the samples prepared with only mechanical mixing (Fig. 2), Nv-6B-M-U-A3 and Nv-10H-M-U-A3 presented limited graphitization, which represents an average GL reduction of about ~54%, respectively (Fig. 3a and b). Such a performance indicated that this preparation procedure (mechanical + ultrasonic mixing) might have a negative impact on the graphitization.

Additionally, a broad hump associated to the disordered carbon phase shows up at ~24° in Fig. 3. The stronger atomic linkages resulting from increased chemical reactions during sonication, hindered ordered structuring of the resultant bonds. Typically, the additional mixing technique can induce high energy chemical reactions due to formation, growth and collapse of bubbles, which favors the release of instantaneous pressure and high-intensity local heating, decreasing the resulting amount of graphitic carbons [57,58]. No significant change took place in the composition containing 10 wt% HMTA, as the presence of HMTA still prevented carbon graphitization (Fig. 3c). To ascertain the conclusion drawn, the analysis was repeated with the same batch of samples as shown in Table 5. Furthermore, introducing the additional mixing technique did not diminish the heterogeneity detected in the prepared compositions.

3.2.2. Effect of vacuum degassing on graphitization level

Degassing of the resin composition prior to pyrolysis produces a similar effect to using ultrasonic mixing. The GL value of novolac resin catalyzed with boron oxide or boric acid significantly decreases with the removal of entrapped gas from the formulation (Fig. 4a and b). Compared to Nv-6B-M-A3 and Nv-10H-M-A3 (Fig. 2), GL values of Nv-6B-M-V-A3 and Nv-10H-M-V-A3 represent an average reduction of 52% and 63%, respectively. According to Pilkenton et al. [59], the presence of oxygen in an organic precursor will inhibit free-radical

Table 5
Comparison of the average graphitization level (GL$_a$) for samples prepared with mechanical mixing or with mechanical + ultrasonic mixing. All materials were fired up to 1000 °C for 5 h and under reducing atmosphere.

Samples	GL$_a$ (%)*
Nv-6B-M-A3	47 ± 10
Nv-6B-M-U-A3	21 ± 7
Nv-10H-M-A3	49 ± 12
Nv-10H-M-U-A3	19 ± 9
Nv-HMTA-10H-M-A3	NS
Nv-HMTA-10H-M-U-A3	NS

* NS = not significant.

Table 6
Comparison of the average graphitization level (GL$_a$) for samples prepared with mechanical mixing and with or without applying vacuum degassing during the processing steps. All materials were fired up to 1000 °C for 5 h and under reducing atmosphere.

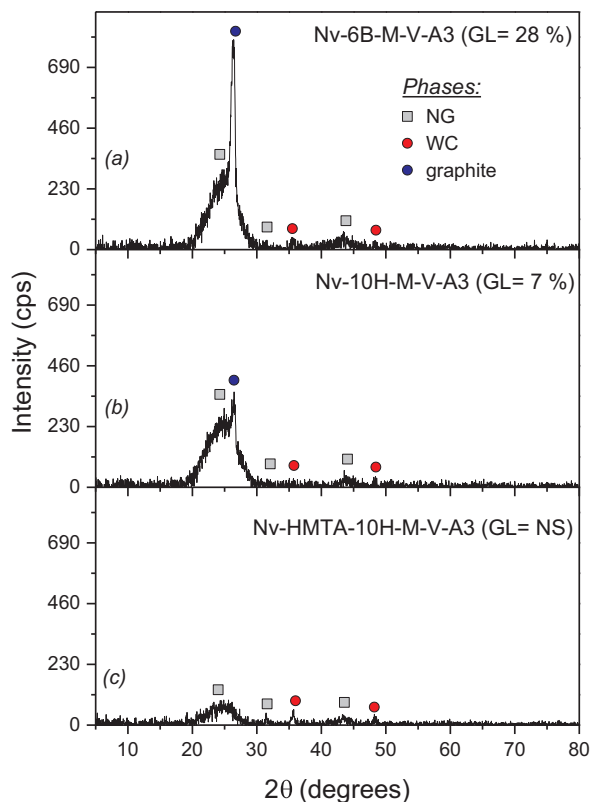| Samples	GL$_a$ (%)*
Nv-6B-M-A3	47 ± 10
Nv-6B-M-V-A3	22 ± 9
Nv-10H-M-A3	49 ± 12
Nv-10H-M-V-A3	15 ± 11
Nv-HMTA-10H-M-A3	NS
Nv-HMTA-10H-M-V-A3	NS

* NS = not significant.

Fig. 4. XRD profiles of the prepared samples showing the effect of vacuum degassing on catalytic graphitization of novolac resin after firing at 1000 °C for 5 h under reducing atmosphere. GL = graphitization level, NS = not significant, A3 = heating procedure at 3 °C/min, M = mechanical mixing, V = vacuum degassing, NG = non-graphitic, WC = tungsten carbide, 6B = 6 wt% B$_2$O$_3$, 10 H = 10 wt% H$_3$BO$_3$, HMTA = 10 wt% hexamethylenetetramine).

polymerization by reacting to form stable peroxy radicals which restrict the degree of conversion and amount of cross-linking network. The aforementioned process can occur at several steps in the reaction sequence leading to an extension in the induction time needed for the completion of polymerization (as they do not readily reinitiate the process). Consequently, the incorporation of vacuum degassing favors increased cross-linking amid curing, which eventually limits the rotation of atoms to graphene layers during carbonization [40].

Additionally, the effect of degasification appears to be more significant when boric acid (compared to boron oxide) was the graphitizing agent. The intermolecular hydrogen bond between H$_3$BO$_3$ and novolac resin may enhance the cross-linkage's effect during the chemical reactions. Besides, with and without the introduction of vacuum degassing, the presence of HMTA in boric acid catalyzed resin hindered its graphitization (Fig. 3c). The results further justify the role of the atoms' binding energy on an ordered rearrangement of carbonized resin

[8,41,60]. Consequently, all factors that favour substantial bonding during the curing stage may inhibit the generation of graphitic carbons from B$_2$O$_3$ or H$_3$BO$_3$ catalyzed resin. Moreover, the results suggest that the initial presence of oxygen may not prevent graphite formation when CCR bricks are fired. The average graphitization results (GL$_a$) of the carbons derived from the compositions prepared with and without the degassing step are presented in Table 6.

3.2.3. Effect of heating rates on the catalytic graphitization of novolac resin with boron compound additives

Generally, the heating rate influences the course of chemical reaction and diffusion process, hence its role on graphitization of the catalyzed resin was investigated. The firing procedures designated as A2, A3, A4 and A5 represent 2, 3, 4 and 5 °C/min heating rates based on A-procedure. The phase evolution of Nv-6B-M and Nv-10H-M compositions under 2–5 °C/min heating rates is shown in Fig. 5. The hump at ∼ 26°, which is related to the graphite phase, gradually appears whereas the amorphous one (near the 002 plane of the graphitic structure) decreases as the heating rate increases from 2 to 3 °C/min (Figs. 5b and 5c). These patterns represent a transition from amorphous to graphitic carbons. In principle, because the pyrolysis operation involves the formation and breaking of bonds, the heating sequence may influence the atoms' binding energy. Therefore, a decrease in the GL values below 3 °C/min may be attributed to the higher cross-linking induced by prolonged HTT during the pre-pyrolysis stage. The strong chemical bonding limits the fusion and the rotation of the atoms during heat treatment [42]. Besides, the use of 4 and 5 °C/min heating rates (Figs. 5d and 5e) restrict catalytic additive diffusion and minimizes bond breaking due to the shorter HTT applied during the pyrolysis operation, which resulted in limited carbon crystallization [8,61].

The XRD profiles of the pyrolytic carbons derived from boric acid-catalyzed resin shows a similar GL evolution (Figs. 5g - 5i). The 3 °C/min heating rate also seems to be the most favorable condition for its catalytic graphitization. The results indicate that any adopted protocol must: (i) not generate substantial cross-linking during pre-pyrolysis stages, (ii) provide enough time for the graphitizing agents to act and, (iii) ensure maximum bond cleavage and atom rearrangement to develop a more ordered structure from the amorphous carbons.

3.2.4. Comparison of the graphitization level induced by boric oxide and boric acid under different heat treatment procedures

To find other factors that might influence or induce Nv graphitization, the effect of different treatment pathways i.e. B3 and C3-procedure (see Table 2) was also evaluated. The selected procedures provided information on the role of the heating sequence and increased HTT during curing (below 500 °C) on the graphite crystallization. The peak's intensity at ∼26° decreased for samples produced via B3 and C3 treatments (Fig. 6). Compared to Nv-6B-M-A3 (GL = 54%), the GL of Nv-6B-M-B3 and Nv-6B-M-C3 decreased to 31.5% and 8%, respectively. Similarly, Nv-10H-M-B3 compared to Nv-10H-M-A3 shows a reduction of about 23% of this property, whereas the GL of Nv-10H-M-C3
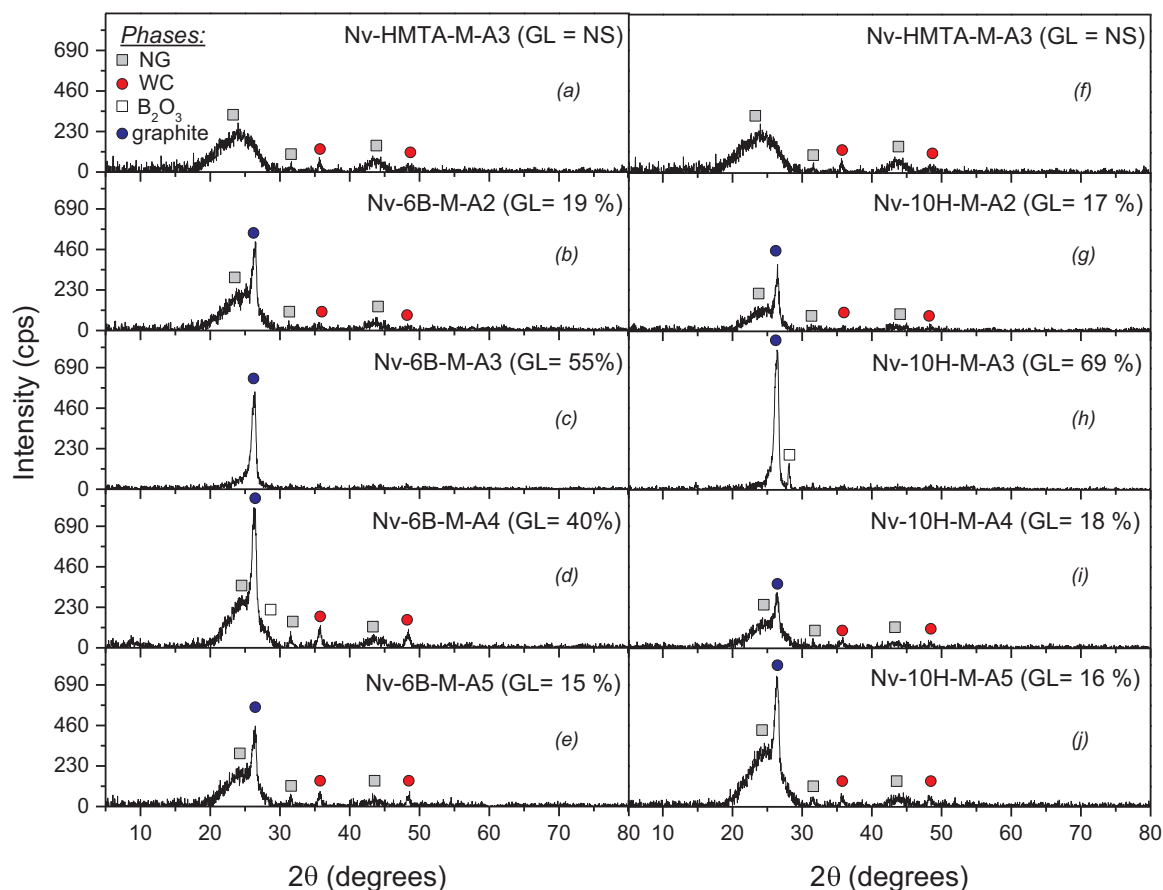
Fig. 5. Effect of heating rates on graphitization of carbonized novolac resin containing: (a) boron oxide or (b) boric acid as graphitizing agent. GL = graphitization level, NS = not significant, M = mechanical mixing, NG = non-graphitic, WC = tungsten carbide, 6B = 6 wt% B_2O_3, 10 H = 10 wt% H_3BO_3, HMTA = 10 wt% hexamethylenetetramine.

becomes insignificant.

The results show that using additional dwell time during the curing stages was not suitable for maximum generation of graphite. Typically, cross-linking degree of resin containing additives depends on specific formulation, cross-linking system, temperature condition, curing time, etc. [62–64]. Both the B3 and C3-procedure might have induced stronger bonding, which gave rise to three-dimensional structure, lower disruption, structuring and maximum graphitization of the catalyzed resin. In a previous study, Liu et al. [65] clearly show, by measuring the glass transition temperature, that the degree of cross-linking in boric acid catalyzed resin increased with prolonged curing time. A similar pattern was pointed out by Luz et al. [44] as the use of a slow curing step resulted in a lower graphitization level of novolac resin composition containing 10 wt% boric acid. Both mentioned experimental results justify the explanation provided earlier. Consequently, the heating sequence was identified as another factor that can affect the graphite generation from B_2O_3 or H_3BO_3 catalyzed novolac resin. Regarding Nv-HMTA-10H composition, no significant phase transition was detected as a result of change in the heating procedures (although the intensity of the broad hump decreases with the B3 or C3-procedure).

4. Conclusions

Boron oxide and boric acid present catalytic ability to induce graphite generation during pyrolysis of novolac resin, which is used as a binder for CCRs. Nv-6B-M and Nv-10H-M formulations, heat treated using A3-procedure, showed the best graphitization level with an average-value of 47% ± 10% and 49% ± 12%, respectively. The interlayer spacing and crystallite height of the carbons prepared in this way were also improved by introducing boron. For example, Nv-10H-M

heat treated up to 1000 °C for 5 h presented $d_{002} = 0.3382 \pm 0.001$ nm and $L_c = 10.66 \pm 2.09$ nm, whereas that of Nv were 0.3742 nm and 1.69 nm, respectively. Furthermore, there is a clear indication that the molecular structure's mobility plays a significant role on the catalytic graphitization of novolac resin by boron oxide and boric acid. The investigation shows that the polymerization degree during initial carbonization stages affects the generated amount of graphite from B_2O_3 or H_3BO_3-catalyzed novolac resin carbons. Consequently, factors such as ultrasonic mixing, vacuum degassing, heating rates that promote stronger cross-linking, limit the breakage of bonds necessary for graphite generation (i.e. they have a negative impact on the graphitization process). Therefore, in CCR development, such processing parameters should be monitored to prevent a higher degree of cross-linking for maximum formation of crystalline carbon from the catalyzed novolac resin binder. This can be achieved by using the A3-procedure as outlined in this study. Moreover, the low pyrolysis temperature (1000 °C) is important because it provides assurance that thermal treatment of the catalyzed novolac resin bonded CCRs will lead to a generation of graphitic structure.

Based on the attained results, higher pyrolysis temperature and prolong holding time, addition of dispersing agents to the catalyzed resin, the use of increased amount of catalytic additives and the synthesis route to achieve homogenous graphitization, will be investigated in a future study. Moreover, accurate quantification of heterogeneous materials comprising amorphous and crystalline products using the XRD technique is typically limited by a lack of homogeneity and the effect of particle size/morphology/distribution leading to errors in the estimated crystallinity degree. Hence, the sample's preparation stage may be modified to improve the homogeneous level of the compositions.
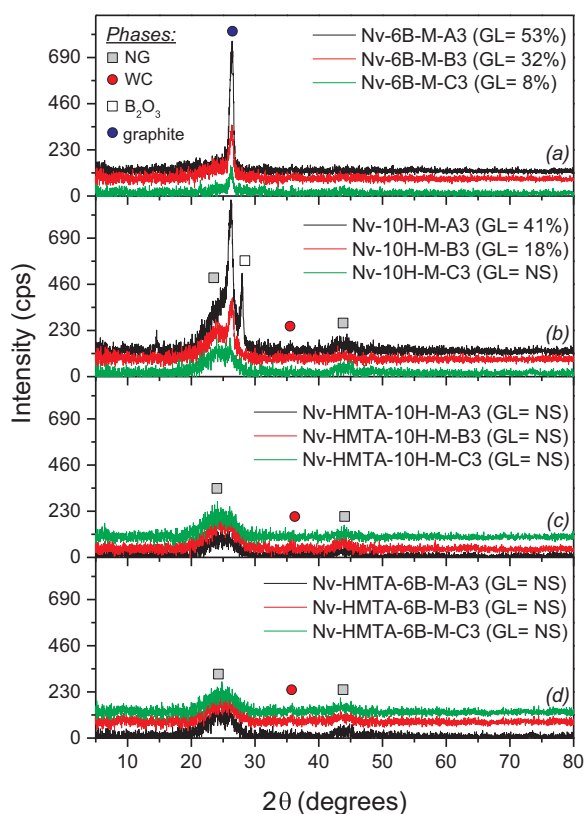
Fig. 6. XRD profiles of the evaluated compositions showing the effect of different heat treatment sequence on graphitization of catalyzed novolac resin after firing at 1000 °C for 5 h under reducing atmosphere. GL = graphitization level, NS = not significant, M = mechanical mixing, NG = non-graphitic, WC = tungsten carbide, 6B = 6 wt% B₂O₃, 10 H = 10 wt% H₃BO₃, HMTA = 10 wt% hexamethylenetetramine.

Regarding the use of boric acid as graphitizing agent, consideration should be given to the refractory aggregate susceptibility to hydration due to water evolution. However, the challenge may not be sufficient to disregard its benefit as its percentage in the entire formulation is small. Moreover, boric acid may also be applied in other resin-containing refractory systems, where MgO would not be present and this hydration effect would not be an issue.

Acknowledgements

References

[1] E.V. Krivokorytov, A.G. Gur'ev, B.I. Polyak, High-carbon binders in refractories and corrosion-resistant ceramics technology, Glass Ceram. 55 (1998) 144–147, http://dx.doi.org/10.1007/bf02694727.
[2] P.L.A. Gardziella, A. Knop, Phenolic Resins: Chemistry, Applications, Standardization, Safety and Ecology, 2nd ed., Springer-Verlag Berlin Heidelberg, New York, 2000, http://dx.doi.org/10.1007/978-3-662-04101-7.
[3] W. Lian, H. Song, X. Chen, L. Li, J. Huo, M. Zhao, G. Wang, The transformation of acetylene black into onion-like hollow carbon nanoparticles at 1000 °C using an iron catalyst, Carbon 46 (2008) 525–530, http://dx.doi.org/10.1016/j.carbon.2007.12.024.
[4] B. Zhu, G. Wei, X. Li, L. Ma, Y. Wei, Structure evolution and oxidation resistance of pyrolytic carbon derived from fe doped phenol resin, in: Proceedings of the Unified International Technical Conference on Refractories (UNITECR 2013), John Wiley & Sons, Inc., pp. 1075–1080, 2013. ⟨http://dx.doi.org/10.1002/9781118837009.ch182⟩.
[5] S.H. Lee, C.C.M. Ma, C.C. Teng, M.Y. Yen, Y.L. Huang, K.C. Yu, Y.H. Yu, I. Wang, The effect of a magnetic field on the graphitization of carbon nanotubes and its application in field emission, Diam. Relat. Mater. 25 (2012) 111–118, http://dx.doi.
[6] S. Xu, F. Zhang, Q. Kang, S. Liu, Q. Cai, The effect of magnetic field on the catalytic graphitization of phenolic resin in the presence of Fe–Ni, Carbon 47 (2009) 3233–3237, http://dx.doi.org/10.1016/j.carbon.2009.07.036.
[7] G.C. Loh, D. Baillargeat, Graphitization of amorphous carbon and its transformation pathways, J. Appl. Phys. 114 (2013) 033534, http://dx.doi.org/10.1063/1.4816313.
[8] C.S. Bitencourt, A.P. Luz, C. Pagliosa, V.C. Pandolfelli, Role of catalytic agents and processing parameters in the graphitization process of a carbon-based refractory binder, Ceram. Int. 41 (2015) 13320–13330, http://dx.doi.org/10.1016/j.ceramint.2015.07.115.
[9] A. Oya, S. Jikihara, S. Otani, Catalytic graphitization of a phenolic resin carbon by nickel (~100 μm): selective gasification of three resultant components as studied by SEM, Fuel 62 (1983) 50–55, http://dx.doi.org/10.1016/0016-2361(83)90252-1.
[10] A. Ōya, S. Ōtani, Catalytic graphitization of carbons by various metals, Carbon 17 (1979) 131–137, http://dx.doi.org/10.1016/0008-6223(79)90020-4.
[11] A. Ōya, R. Yamashita, S. Ōtani, Catalytic graphitization of carbons by borons, Fuel 58 (1979) 495–500, http://dx.doi.org/10.1016/0016-2361(79)90167-4.
[12] R. Imamura, K. Matsui, S. Takeda, J. Ozaki, A. Oya, A new role for phosphorus in graphitization of phenolic resin, Carbon 37 (1999) 261–267, http://dx.doi.org/10.1016/S0008-6223(98)00172-9.
[13] E.M. Wewerka, R.J. Imprescia, The use of organometallic additives to promote graphitization of carbons derived from furfuryl alcohol resins, Carbon 11 (1973) 289–297, http://dx.doi.org/10.1016/0008-6223(73)90069-9.
[14] A.S. Gokce, C. Gurcan, S. Ozgen, S. Aydin, The effect of antioxidants on the oxidation behaviour of magnesia–carbon refractory bricks, Ceram. Int. 34 (2008) 323–330, http://dx.doi.org/10.1016/j.ceramint.2006.10.004.
[15] C.G. Aneziris, J. Hubálková, R. Barabás, Microstructure evaluation of MgO–C refractories with TiO₂- and Al-additions, J. Eur. Ceram. Soc. 27 (2007) 73–78, http://dx.doi.org/10.1016/j.jeurceramsoc.2006.03.001.
[16] S. Wang, X. Jing, Y. Wang, J. Si, High char yield of aryl boron-containing phenolic resins: the effect of phenylboronic acid on the thermal stability and carbonization of phenolic resins, Polym. Degrad. Stab. 99 (2014) 1–11, http://dx.doi.org/10.1016/j.polymdegradstab.2013.12.011.
[17] S. Wang, Y. Wang, C. Bian, Y. Zhong, X. Jing, The thermal stability and pyrolysis mechanism of boron-containing phenolic resins: the effect of phenyl borates on the char formation, Appl. Surf. Sci. 331 (2015) 519–529, http://dx.doi.org/10.1016/j.apsusc.2015.01.062.
[18] J.P. Guha, J.D. Smith, Reaction chemistry and microstructure development of MgO-C refractories containing metal antioxidants, in: Proceedings of the Unified International Technical Conference on Refractories (UNITECR 2005), Orlando, USA, 2005, pp. 97–99.
[19] H.A. Al-Falahi, Catalytic graphitization of modified phenolic resin and its nanoparticles fillers behavior towards high temperature, Adv. Mater. Res. 925 (2014) 282–289, http://dx.doi.org/10.4028/www.scientific.net/AMR.925.282.
[20] Y.Z. Biao LI, Z. Zheng, X. Zhao, Characterization of boron modified phenolic resin and its curing behavior, Adv. Mater. Res. 233–235 (2011) 137–141, http://dx.doi.org/10.4028/www.scientific.net/AMR.233-235.137.
[21] P. Xu, X. Jing, High carbon yield thermoset resin based on phenolic resin, hyperbranched polyborate, and paraformaldehyde, Polym. Adv. Technol. 22 (2011) 2592–2595, http://dx.doi.org/10.1002/pat.1806.
[22] Y. Liu, X. Jing, Pyrolysis and structure of hyperbranched polyborate modified phenolic resins, Carbon 45 (2007) 1965–1971, http://dx.doi.org/10.1016/j.carbon.2007.06.008.
[23] C. Martín, J.C. Ronda, V. Cádiz, Boron-containing novolac resins as flame retardant materials, Polym. Degrad. Stab. 91 (2006) 747–754, http://dx.doi.org/10.1016/j.polymdegradstab.2005.05.025.
[24] J. Wang, N. Jiang, H. Jiang, Micro-structural evolution of phenol-formaldehyde resin modified by boron carbide at elevated temperatures, Mater. Chem. Phys. 120 (2010) 187–192, http://dx.doi.org/10.1016/j.matchemphys.2009.10.044.
[25] S. Zhang, A. Yamaguchi, Effects of B₄C on the crystallization and oxidation resistance of carbon from resin, J. Ceram. Soc. Jpn. 102 (1994) 830–834.
[26] N. Liao, Y. Li, S. Jin, S. Sang, G. Liu, Reduced brittleness of multi-walled carbon nanotubes (MWCNTs) containing Al₂O₃-C refractories with boron carbide, Mater. Sci. Eng. A 698 (2017) 80–87.
[27] S. Wang, X. Jing, Y. Wang, J. Si, Synthesis and characterization of novel phenolic resins containing aryl-boron backbone and their utilization in polymeric composites with improved thermal and mechanical properties, Polym. Adv. Technol. 25 (2014) 152–159, http://dx.doi.org/10.1002/pat.3216.
[28] J. Simitzis, L. Zoumpoulakis, Influence of FeCl₃ dopant on the electrical conductivity of pyrolysed aromatic polymers, J. Mater. Sci. 31 (1996) 1615–1620, http://dx.doi.org/10.1007/bf00357872.
[29] L. Liu, Z. Ye, Effects of modified multi-walled carbon nanotubes on the curing behavior and thermal stability of boron phenolic resin, Polym. Degrad. Stab. 94 (2009) 1972–1978, http://dx.doi.org/10.1016/j.polymdegradstab.2009.07.022.
[30] S. Theodoropoulou, D. Papadimitriou, L. Zoumpoulakis, J. Simitzis, Structural and optical characterization of pyrolytic carbon derived from novolac resin, Anal. Bioanal. Chem. 379 (2004) 788–791, http://dx.doi.org/10.1007/s00216-003-2453-5.
[31] H. Jansen, Bonding of MgO-C bricks by catalytically activated resin, Millenn. Steel Int. (2007) 95–98.
[32] G.S. Rellick, Carbon and Graphite Matrices in Carbon-carbon Composites: an Overview of Their Formation, Structure, and Properties, DTIC Document, 1992.
[33] R. Hu, T.C. Chung, Synthesis and characterization of novel B/C materials prepared by 9-chloroborafluorene precursor, Carbon 34 (1996) 1181–1190, http://dx.doi.org/10.1016/0008-6223(96)00064-4.

[34] L.E. Jones, A. Throwerp, Influence of boron on carbon fiber microstructure, physical properties, and oxidation behavior, Carbon 29 (1991) 251–269, http://dx.doi.org/10.1016/0008-6223(91)90076-U.

[35] L. Pilato, Phenolic Resins: A Century of Progress, Springer Berlin Heidelberg, 2010.

[36] J.W. Martin, Concise Encyclopedia of the Structure of Materials, Elsevier Science, 2006.

[37] R.E. Franklin, Crystallite growth in graphitizing and non-graphitizing carbons, Proc. R. Soc. London. Ser. A. Math. Phys. Sci. 209 (1951) 196–218.

[38] R.L. Beatty, Graphitization Kinetics of Fluidized-bed Pyrolytic Carbons, 1974.

[39] A. Oberlin, M. Oberlin, Graphitizability of carbonaceous materials as studied by TEM and X-ray diffraction, J. Microsc. 132 (1983) 353–363, http://dx.doi.org/10.1111/j.1365-2818.1983.tb04600.x.

[40] J.J. Kipling, J.N. Sherwood, P.V. Shooter, N.R. Thompson, Factors influencing the graphitization of polymer carbons, Carbon 1 (1964), pp. 315–320, http://dx.doi.org/10.1016/0008-6223(64)90285-4.

[41] J.J. Kipling, P.V. Shooter, R.N. Young, The effect of sulphur on the graphitization of carbons derived from polyvinyl chloride-sulphur systems, Carbon 4 (1966) 333–341, http://dx.doi.org/10.1016/0008-6223(66)90046-7.

[42] J.J. Kipling, P.V. Shooter, Factors affecting the graphitization of carbon: evidence from polarized light microscopy, Carbon 4 (1966) 1–4, http://dx.doi.org/10.1016/0008-6223(66)90003-0.

[43] J. Yun, L. Chen, X. Zhang, J. Feng, L. Liu, The effect of introducing B and N on pyrolysis process of high ortho novolac resin, Polymers 8 (2016) 1–17, http://dx.doi.org/10.3390/polym8030035.

[44] A.P. Luz, C.G. Renda, A.A. Lucas, R. Bertholdo, C.G. Aneziris, V.C. Pandolfelli, Graphitization of phenolic resins for carbon-based refractories, Ceram. Int. 43 (2017) 8171–8182, http://dx.doi.org/10.1016/j.ceramint.2017.03.143.

[45] C.A. Lytle, W. Bertsch, M. McKinley, Determination of novolac resin thermal decomposition products by pyrolysis-gas chromatography-mass spectrometry, J. Anal. Appl. Pyrolysis 45 (1998) 121–131, http://dx.doi.org/10.1016/S0165-2370(98)00062-X.

Guyer and Rowell, 1967 [46] V.L. Guyer, V.M. Rowell, Liquid Boric Acid Suspension, Method and Products, Google Patents, US 3306860 A, EUA, 1967.

[47] D. Balzar, X-ray diffraction line broadening: modeling and applications to high-Tc superconductors, J. Res. Nat. Inst. Stand. Tech. 98 (1993) 321–351.

[48] R.E. Franklin, Homogeneous and Heterogeneous Graphitization of Carbon, Nature 177 (1956) (239-239).

[49] K. Okabe, S. Shiraishi, A. Oya, Mechanism of heterogeneous graphitization observed in phenolic resin-derived thin carbon fibers heated at 3000 °C, Carbon 42 (2004) 667–669, http://dx.doi.org/10.1016/j.carbon.2003.11.018.

[50] K. Kamiya, K. Suzuki, Preferential alignment of carbon layers around pores in hard carbon and multi-phase graphitization, Carbon 13 (1975) 317–320, http://dx.doi.org/10.1016/0008-6223(75)90036-6.

[51] M. Sevilla, A.B. Fuertes, Catalytic graphitization of templated mesoporous carbons, Carbon 44 (2006) 468–474, http://dx.doi.org/10.1016/j.carbon.2005.08.019.

[52] T.H. Ko, W.S. Kuo, Y.H. Chang, Microstructural changes of phenolic resin during pyrolysis, J. Appl. Polym. Sci. 81 (2001) 1084–1089, http://dx.doi.org/10.1002/app.1530.

[53] J.S. Burgess, C.K. Acharya, J. Lizarazo, N. Yancey, B. Flowers, G. Kwon, T. Klein, M. Weaver, A.M. Lane, C. Heath Turner, S. Street, Boron-doped carbon powders formed at 1000 °C and one atmosphere, Carbon 46 (2008) 1711–1717, http://dx.doi.org/10.1016/j.carbon.2008.07.022.

[54] X. Zhang, D.H. Solomon, Carbonization reactions in novolac resins, hexamethylenetetramine, and furfuryl alcohol mixtures, Chem. Mater. 11 (1999) 384–391, http://dx.doi.org/10.1021/cm980605i.

[55] T. Enoki, M. Suzuki, M. Endo, Graphite Intercalation Compounds and Applications, Oxford University Press, 2003.

[56] M.B. Vázquez-Santos, E. Geissler, K. László, J.-N. Rouzaud, A. Martínez-Alonso, J.M.D. Tascón, Comparative XRD, Raman, and TEM study on graphitization of pbo-derived carbon fibers, J. Phys. Chem. C 116 (2012) 257–268, http://dx.doi.org/10.1021/jp2084499.

[57] S.-G. Zhao, B.-C. Wang, Q. Sun, Effect of physical disturbance on the structure of needle coke, Chin. Phys. B 19 (2010) 1–5.

[58] K.S. Suslick, W.L. Nyborg, Ultrasound: its chemical, physical and biological effects, J. Acoust. Soc. Am. 87 (1990) 919–920.

[59] M. Pilkenton, J. Lewman, R. Chartoff, Effect of oxygen on the crosslinking and mechanical properties of a thermoset formed by free-radical photocuring, J. Appl. Polym. Sci. 119 (2011) 2359–2370, http://dx.doi.org/10.1002/app.32650.

[60] I.A.S. Edwards, H. Marsh, Introduction to Carbon Science, Butterworths, 1989.

[61] J.C.J. Bart, Polymer Additive Analytics: Industrial Practice And Case Studies, Firenze University Press, 2006.

[62] C. Zhao, G. Zhang, L. Zhao, Effect of curing agent and temperature on the rheological behavior of epoxy resin systems, Molecules 17 (2012) 8587–8594.

[63] B. Kandola, J. Ebdon, K. Chowdhury, Flame retardance and physical properties of novel cured blends of unsaturated polyester and furan resins, Polymers 7 (2015) 298–315.

[64] G. Manikandan, K. Bogeshwaran, Effect of curing time on phenolic resins using latent acid catalyst, Int. J. ChemTech Res. 9 (2016) 30–37.

[65] Y. Liu, J. Gao, R. Zhang, Thermal properties and stability of boron-containing phenol-formaldehyde resin formed from paraformaldehyde, Polym. Degrad. Stab. 77 (2002) 495–501, http://dx.doi.org/10.1016/S0141-3910(02)00107-6.